Amperometric Biosensor Based on Cu2O@Au Nanocomposites for the Detection of Galectin-1 via Lactose-Galectin Interactions

To cite this article before publication: Feng Long *et al* 2019 *Nanotechnology* in press https://doi.org/10.1088/1361-6528/ab3cde

IOP Publishing Nanotechnology
Nanotechnology **XX** (XXXX) XXXXXX https://doi.org/XXXX/XXXX

Amperometric Biosensor Based on Cu_2O@Au Nanocomposites for the Detection of Galectin-1 via Lactose-Galectin Interactions

Feng Long[1,2,5], Wei Li[1,5] , Wanling Chen[1], Danni Liu[1], Yue Chen[2,4], Rui Zhou[3,4], Penghui Li[1,4]

[1] Shenzhen Institutes of Advanced Technology, Chinese Academy of Sciences, Shenzhen 518055, China;
[2] Department of Medical Laboratory, The Second Clinical Medical College (Shenzhen People's Hospital), Jinan University, Shenzhen 518020, China
[3] Department of Engineering Physics, Tsinghua University, Beijing 100084, China

E-mail: chenyue_dr@163.com; zhour@tsinghua.edu.cn; ph.li@siat.ac.cn

Received xxxxxx
Accepted for publication xxxxxx
Published xxxxxx

Abstract

In this work, a novel label-free electrochemical biosensor is developed for the detection of galectin-1 (Gal-1) based on the gold nanoparticles (AuNPs) loaded octahedral Cu_2O (Cu_2O@Au) nanocomposites. The AuNPs on the surface of Cu_2O nanocrystals not only enhance the electrochemical performance, but also can serve as the binding sites for lactose ligand which can specifically bind with Gal-1. The Cu_2O@Au nanocomposites provide the synergic effect of electrochemical signal amplification and lactose-galectin reaction as the recognition strategy. Under the optimal conditions, the proposed biosensor exhibit variations of electrochemical responses to different concentrations of Gal-1 ranging from 0.1 pg/mL to 10 ng/mL. This work presents an alternative of electrochemical biosensor for the detection of tumor biomarker based on simply and economically lactose ligand incorporated Cu_2O@Au biosensor platform..

Keywords: Galectin-1, nanocomposites, electrochemical biosensor, lactose ligand, detection

1. Introduction

Tumor markers are the molecules existed in blood, urine, or body tissues, whose identification and determination are of great importance in oncology, especially for the early-stage screening of cancers [1]. Galectin-1 (Gal-1) is a prototype member of the galectins family of glycan-binding proteins, which plays a major role in the progression of different tumors [2,3]. There are widespread reports about the overexpression of Gal-1 in human cancer, including thyroid cancer [4], epithelial ovarian cancer [5], chondroblastic osteosarcoma [6], pancreatic ductal adenocarcinoma [7,8], and oral squamous cell carcinoma [9]. Thus, Gal-1 is a broad-spectrum biomarker of tumors, and it is crucial to develop rapid, accurate, and convenient analytical techniques for screening and clinical diagnosis of cancers via Gal-1 detection.

The detection of Gal-1 for diagnosing tumors is arisen in recent years, which is mainly implemented with the methods like matrix-assisted laser desorption/ionization-time of flight-

[4] Authors to whom any correspondence should be addressed.
[5] These authors contributed equally to this work.

mass spectrometry (MALDI-TOF-MS) [10], fluoroimmunoassay [4] and enzyme-linked immunosorbent assay (ELISA) [5]. Nevertheless, these strategies suffer from either instrumental sophistication or time-consuming process.

Recently, the bioassays based on the direct electronic signal responses of electrochemical biosensors have been widely used to detect tumor biomarkers, such as prostate specific antigen [11], α-fetoprotein [12] and carcinoembryonic antigen [13], due to the ease of operation, fast response, relative low cost and miniaturization feasibility. So far, most of these electrochemical biosensors are immunosensors regarding the specific responses between antigens and antibodies. Actually, galectins are a sub-family of lectins with a conserved carbohydrate recognition domain (CRD) that can interact with beta-galactosides [14–16]. Various glycoconjugate ligands, for instance lactose has been reported to recognize Gal-1 via galectin-beta-galactosides interaction [17]. Hence in our study, electrochemical biosensor based on lactose-Gal-1 interaction is proposed for the sensitive detection of Gal-1.

The electrode materials are essential for the design and construction of electrochemical biosensors, and with the rapid development of nanotechnology, a variety of nanomaterials with reversible redox activity have been used for modifying the electrode as the electron mediators, such as metal oxides [18], semiconductors [19], and noble metal nanoparticles [20, 21]. In particular, cuprous oxide (Cu_2O) nanocrystals have been widely used to fabricate electrochemical biosensors due to the promising electrical catalytic characteristics, large surface area as well as amenability of shape-controlled synthesis [22] Among the noble metal nanoparticles, gold nanoparticles (AuNPs) are superior for the auxiliary catalytic activity and abundant binding sites [23]. The combination of Cu_2O nanocrystals and AuNPs can efficiently increase the electron transfer efficiency and enhance the electrochemical signal by a synergistic effect [24, 25]. Via this signal amplification strategy, the resultant Cu_2O@Au nanocomposites show the better performance than monometallic counterparts as the electrochemical biosensors.

Based on the specific galectin-lactose recognition, we propose an innovative label-free electrochemical biosensor in this study for the detection of tumor biomarker Gal-1 by using Cu_2O@Au as the transducing materials (Figure 1). The application of Cu_2O@Au not only provides a good deal of active sites for binding sulfhydryl lactose ligands, but also accelerates the electro transfer rate to improve the sensitivity of biosensors. In addition, the lactose ligand used to fabricate biosensor is easy to prepare and economical. The proposed biosensor is sensitive for the detection of Gal-1 via the specific binding between macromolecular proteins and small molecular sugar ligands, hence hold great potential applications for the rapid screening of cancer.

2. Experimental

2.1 Materials

Copper(II) nitrate hydrate ($Cu(NO_3)_2 \cdot 3H_2O$), polyvinyl pyrrolidone (PVP), hydrazine monohydrate ($N_2H_4 \cdot H_2O$), sodium hydroxide (NaOH), and chloroauric acid ($HAuCl_4$), N,N-Dimethylformamide (DMF) (>99.9%), acetic unhydride (Ac_2O), sodium acetate (NaOAc), boron trifluoride diethyl etherate ($BF_3 \cdot Et_2O$), potassium thioacetate (KSAc), sodium methoxide (MeONa), methyl (MeOH) and PBS were purchased from Aladdin chemicals (Shanghai, China). KCl, $K_3[Fe(CN)_6]$, ethanol and sulfuric acid were obtained from

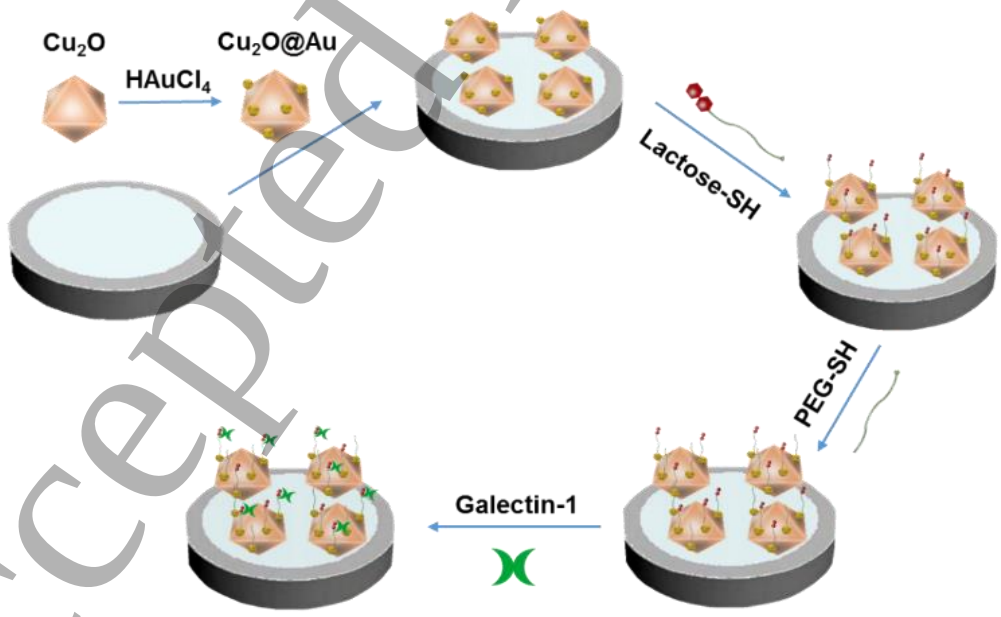

Figure 1. Schematic illustration of the fabrication process of the electrochemical biosensor.

Sigma-Aldrich (Beijing, China). Galectin-1 was bought from PeproTech (Suzhou, China). All the chemicals were used as-received without further purification if not specific otherwise. Millipore™ Milli-Q water (resistivity >18 MΩ cm^{-1} at 25 ℃) was used throughout the experiments.

2.2 Preparation of the lactose ligand

The sulfhydryl lactose ligand (Lactose-SH) was synthesized by the method described previously [26] and the preparation process was shown in Figure S1. Firstly, D-lactose was treated in a mixture of Ac_2O and NaOAc under reflux, giving the peracetylated lactose 1. Subsequently, peracetate 1 proceeded a glycosylation with 2-[2-(2-chloroethoxy)ethoxy]ethanol under the promotion of $BF_3.Et_2O$ to obtain glycoside 2, which was further reacted with potassium thioacetate in DMF to give thioacetate 3. Compound 3 was eventually deacetylated by a catalytic amount of sodium methoxide in methanol, producing the final sulfhydryl lactose ligand 4, which was directly used as prepared.

2.3 Preparation of Cu_2O nanocrystals and Cu_2O@Au nanocomposites

Cu_2O nanocrystals were synthesized by the method previously reported with some modifications [27]. In brief, 0.0048 g of $Cu(NO_3)_2{\cdot}3H_2O$, 12 mL of isopropanol and 0.04 g of polyvinyl pyrrolidone (PVP K30) were mixed by stirring, then NaOH aqueous solution (0.012 g/mL, 1 mL) was added dropwise to the mixed solution. After 10 min of stirring, $N_2H_2{\cdot}H_2O$ (35%, 80 μL) was added dropwise to the aqueous solution. The mixture was stirred 10 min at room temperature. The prepared samples were collected by centrifugation (10000 rpm, 10 min), and then thoroughly washed with absolute ethanol to remove the impurities. Finally, the obtained solid material (Cu_2O) was dried in vacuum at room temperature. For the preparation of Cu_2O@Au nanocomposites, the dried Cu_2O nanocrystals were dispersed in 3.5 mL ultrapure water, and 3 mL of the Cu_2O solution and $HAuCl_4$ (5 mM, 250 μL) were mixed with stirring for 5 min. Subsequently, the prepared solid materials were rinsed thrice by absolute ethanol and centrifugation to remove impurities. Finally, the obtained Cu_2O@Au nanocomposites were dispersed in absolute ethanol for further use. The reaction for Cu_2O@Au formation is as follows:[28]

$$3Cu_2O + 2AuCl_4^- + 6H^+ = 6Cu^{2+} + 2Au + 3H_2O + 8Cl^-$$

2.4 Fabrication of the biosensors

The label-free electrochemical biosensors were fabricated as the process illustrated in Figure 1. Generally, the glassy carbon electrode (GCE) was polished carefully to a mirror-like surface by Al_2O_3 powder with particle size of 0.05 μm, and thoroughly washed by ultrapure water and ethanol. The prepared GCE was coated with Cu_2O@Au (6 μL) and dried in the air. Following that, the resultant electrode was incubated with lactose ligand (6 μL, 10 ng/mL) and dried at room temperature. After washing, the resulting electrode was incubated with thiol-polyethylene glycol (PEG-SH) (6 μL, 10 mg/mL) for 1 h to block nonspecific binding sites. Subsequently, the electrode was washed thoroughly with ethanol and PBS to remove the excess PEG-SH. The proposed electrode after drying was incubated with the different concentrations of Gal-1 (0.1 pg/mL~10 ng/mL, 6 μL) to allow the reaction between ligand and Gal-1. Finally, the electrode was washed extensively to remove unbounded molecules and stored at 4°C for usage.

2.5 Electrochemical measurements

All the electrochemical measurements were carried out on CHI760E electrochemical work station (Shanghai CH Instruments Co, China) using a three-electrode system consisted of a modified GCE (3 mm in diameter) as the working electrode, a platinum wire as the counter electrode, and a saturated calomel electrode (SCE) as the reference electrode. The PBS (pH=7.0) was used as base solvent and electrolyte for all the electrochemical measurements. Cyclic voltammetry (CV) experiments towards 5 mM $K_3[Fe(CN)_6]$ solution containing 0.1 M KCl were performed by scanning the potential from -0.4V to 0.6V at 100 mV/s, and the CV experiments towards H_2O_2 were conducted by scanning the potential from -0.2V to 0.6V at 100 mV/s. The alternating current (A.C.) impedance measurements were conducted with frequency ranging from 0.01 to 10^5 Hz in the same electrolyte. The differential pulse voltammetry (DPV) experiments was conducted by scanning the potential from 0.3 V to 1.0 V in PBS solution (pH=7.0).

2.6 Characterization

The SEM images of the nanocrystals and nanocomposites were acquired on a Sigma (Zeiss, Germany) field-emission scanning electron microscope. X-ray photoelectron spectroscopy (XPS) was conducted on the ESCALAB 250Xi XPS system (Thermo Fisher, USA). The X-ray diffraction patterns were recorded on a D8 Advance X-ray diffractometer (Bruker, Germany).

3. Results and discussion

3.1. Characterizations of Cu_2O nanocrystals and Cu_2O@Au nanocomposites

The morphology and structure of the Cu_2O@Au nanocomposites are investigated and compared with the Cu_2O nanocrystals. Figure 2a and 2b show the SEM images of these two nanoparticles. The synthesized Cu_2O nanocrystals exhibit uniform and homogeneous octahedral shape with an average

diameter of approximately 450 nm (Figure 2a). The surface of the octahedral Cu_2O is quite smooth and neat. With the oxidation-reduction reaction occurred on the surface of Cu_2O nanocrystals, the AuNPs grow evenly onto Cu_2O, suggesting the successful synthesis of Cu_2O@Au nanocomposites. The Cu_2O@Au nanocomposites still maintain the uniform and homogenous shape with only rougher surface (Figure 2b), which might contribute to larger surface area. XPS is further employed to confirm the chemical structure, and the spectra show that the major peaks of Cu_2O at 2θ = 36.52º, 42.42º, 61.55º and 73.73º corresponding to (111), (200), (220) and (311) planes, which match well with octahedral Cu_2O [32]. The XRD pattern of Cu_2O@Au also exhibit the characteristic peaks of Cu_2O, with additional major peaks of Au at 2θ =38.18º, 44.3º, 64.5º, attributing to (111), (200) and (311) planes. Taken together, the results indicate the successful growth of AuNPs onto octahedral Cu_2O.

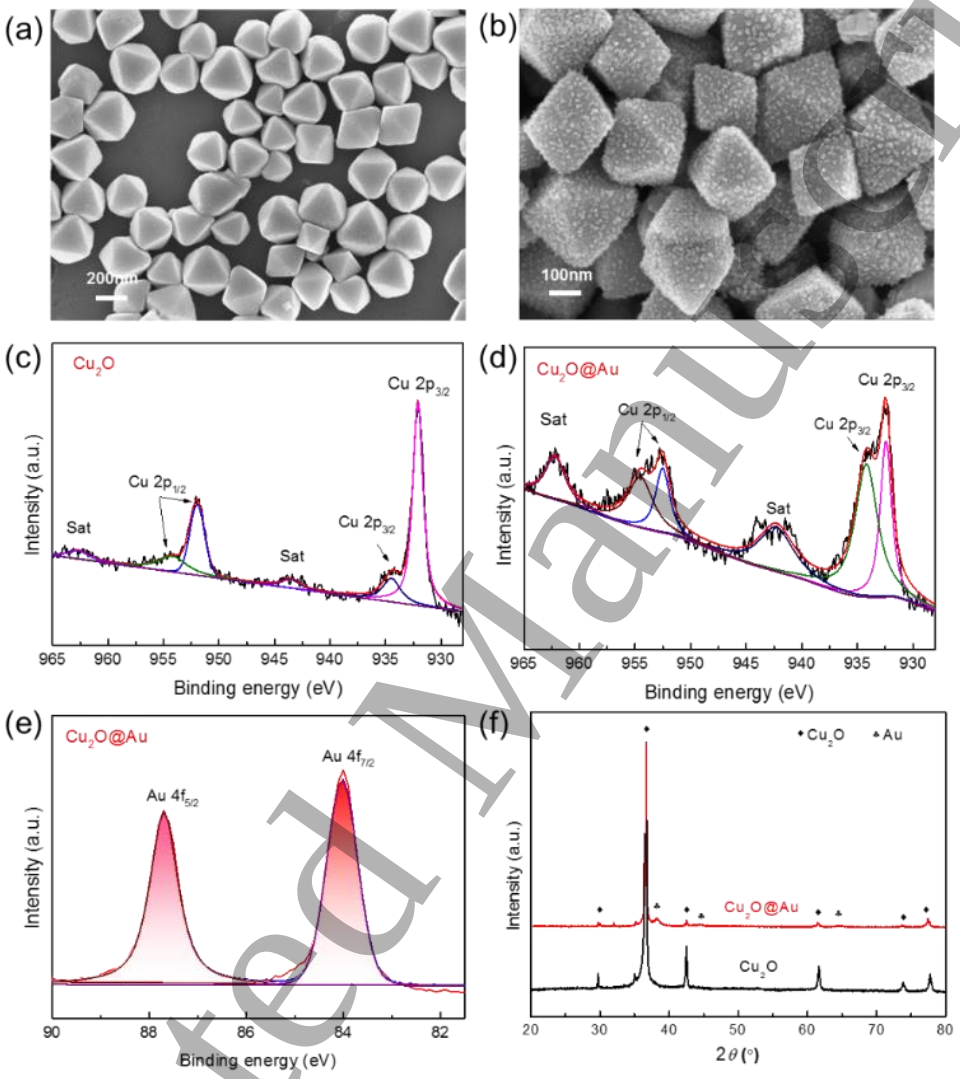

Figure 2. SEM images of Cu_2O (a) and Cu_2O@Au (b); XPS Cu 2p spectra of Cu_2O (c) and Cu_2O@Au (d); Au 4f spectra of Cu_2O@Au (e); XRD patterns of Cu_2O and Cu_2O@Au (f).

are displayed in Figure 2c-2e. The Cu 2p spectrum of Cu_2O (Figure 1c) reveals two main peaks at 932.25 and 952.15 eV, corresponding to the Cu $2p_{3/2}$ and Cu $2p_{1/2}$ peaks of Cu(I) and/or Cu(0), respectively[29,30]. Additionally, the other XPS peaks located at 940.5 and 960.2 eV are the satellite peaks [31]. Noteworthily, even though the Cu 2p spectrum of Cu_2O@Au (Figure 2d) contains the similar peaks, the intensity of peaks is stronger, and Cu_2O@Au is featured for two Au 4f peaks at 87.6 and 83.8 eV (Figure 1e). XRD results (Figure 2f)

3.2 Comparison of the electro-catalytic properties between Cu_2O nanocrystals and Cu_2O@Au nanocomposites

In the measurement of electrochemical biosensor, the catalytic activity and conductivity are important for the sensitivity. Control experiments of CV current response are carried out to determine the catalytic activity of different materials for the catalysis towards 5 M H_2O_2. As shown in Figure 3a, response

curves in electrolyte and those with the addition of 5 M H_2O_2 are obtained from GCE modified with Cu_2O and Cu_2O@Au. By adding H_2O_2, the redox current of Cu_2O nanocrystals increases from 49.8 μA (i) to 53.08 μA (ii), while the redox current of Cu_2O@Au nanocomposites increases from 58.03 μA (iii) to 62.56 μA (iv). It indicates that Cu_2O@Au nanocomposites exhibit better catalytic performance than Cu_2O nanoscystals. The loaded AuNPs with excellent electronic conduction features are in association with the Cu_2O substrates to improve the electrocatalytic property of nanocomposites.

The strategy for electrochemical biosensing of Gal-1 is based on the galectin-lactose interaction, and the fabricated biosensors for Gal-1 recognition are illustrated in Figure 4a. In particular, the Lactose-SH molecules are introduced onto the surface of Cu_2O@Au by gold-sulfur bonding, and PEG-SH molecules are used to block the nonspecific binding sites. It is proposed that the Lactose-SH on the surface of biosensor can specifically capture Gal-1 by recognizing the carbohydrate recognition domain (CRD) of Gal-1. In this respect, the constructed biosensor can be used to detect Gal-1 by monitoring the change of electrochemical performance. In

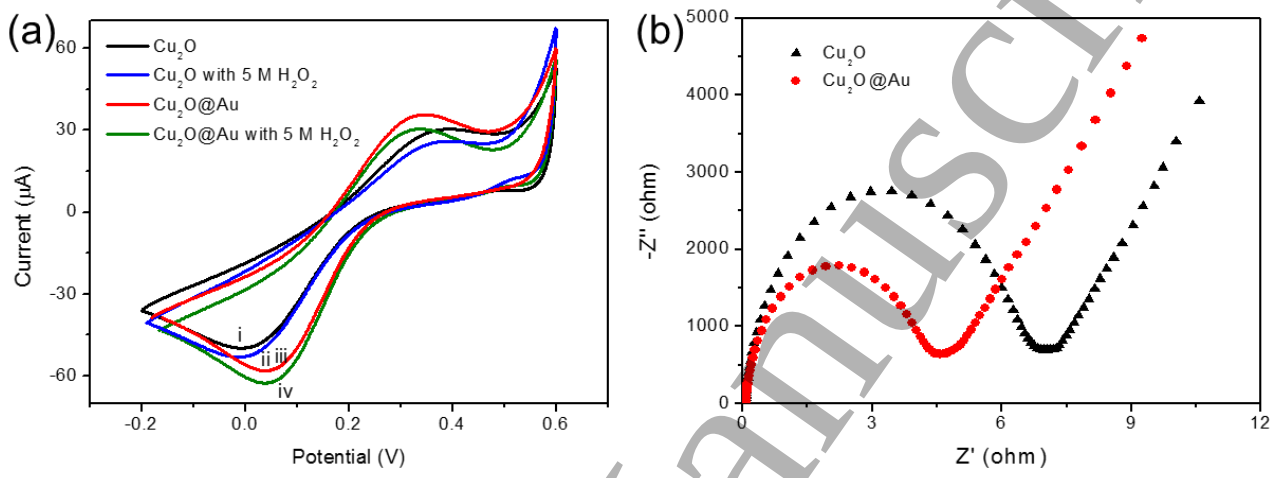

Figure 3. (**a**) The current responses of different modified electrodes in 10 mL eletrolyte (pH=7.0): (i) Cu_2O, (iii) Cu_2O@Au, and those in electrolyte with addition of H_2O_2 (5 M, 10 μL): (ii) Cu_2O, (iv) Cu_2O@Au; (**b**) Nyquist plots of the Cu_2O and Cu_2O@Au modified electrodes with A.C. impedance measurement in a solution containing 0.1M KCl and 5 mM $K_3[Fe(CN)_6]$ at potential of 0.20V with frequency range of 0.1-10^5 Hz.

A.C. impedance measurements can give the information monitoring the interfacial properties and the changes of electron transfer resistance (Ret), from which the semicircle portion at higher frequencies in the Nyquist plots of electrochemical impedance spectroscopy (EIS) indicates the electron transfer limited process and the semicircle diameter corresponds to Ret [33]. Herein, electrical conductivity of the Cu_2O and Cu_2O@Au are investigated by A.C. impedance measurement in a solution containing 0.1 mol/L KCl and 5 mmol/L $K_3[Fe(CN)_6]$. As shown in Figure 3b, the semicircle portion of Cu_2O@Au is much smaller than that of Cu_2O, indicating that Cu_2O@Au has better electric conductivity than Cu_2O. The enhanced electrical conductivity of Cu_2O@Au can be ascribed to that AuNPs serve as electron mediators to significantly improve the electrical conductivity and the electron transfer rate of Cu_2O electrode. Thus, A.C. impedance measurement confirms that the Cu_2O@Au nanocomposites is superior to Cu_2O for the further construction of electrochemical biosensors.

3.3 Electrochemical characterizations of the stepwise-fabricated biosensors

a next step, the biosensor obtained is characterized by EIS and CV measurements with the detection parameters being further optimized.

EIS and CV responses are measured to investigate the stepwise-fabrication of the biosensor and the results are displayed in Figure 4b and 4c. In the PBS (pH=7.0) solution containing 5 mM $K_3[Fe(CN)_6]$ and 0.1 M KCl, the electrode coated with Cu_2O@Au exhibits a relatively small Ret (i). With the binding of Lactose-SH ligand onto the modified electrode surface, the semicircle diameter decreases obviously (ii) due to the better electrical transport properties. The Ret increases significantly after the electrode being blocked with PEG-SH (iii), and increase further after incubation with 10 ng/mL Gal-1, implying the successful capturing of Gal-1 by Lactose-SH. The corresponding CV curves are also recorded as shown in Figure 4c, since CV response is regarded as an effective method for probing the interfacial properties of surface-modified electrodes during the process of fabrication [34]. When the bare GCE is coated with Cu_2O@Au, the redox peak current is 44.19 μA (i), and it obviously increases to 50.03 μA (ii) after binding Lactose-SH ligand onto Cu_2O@Au. Noteworthily, the redox peak current gradually decreases to

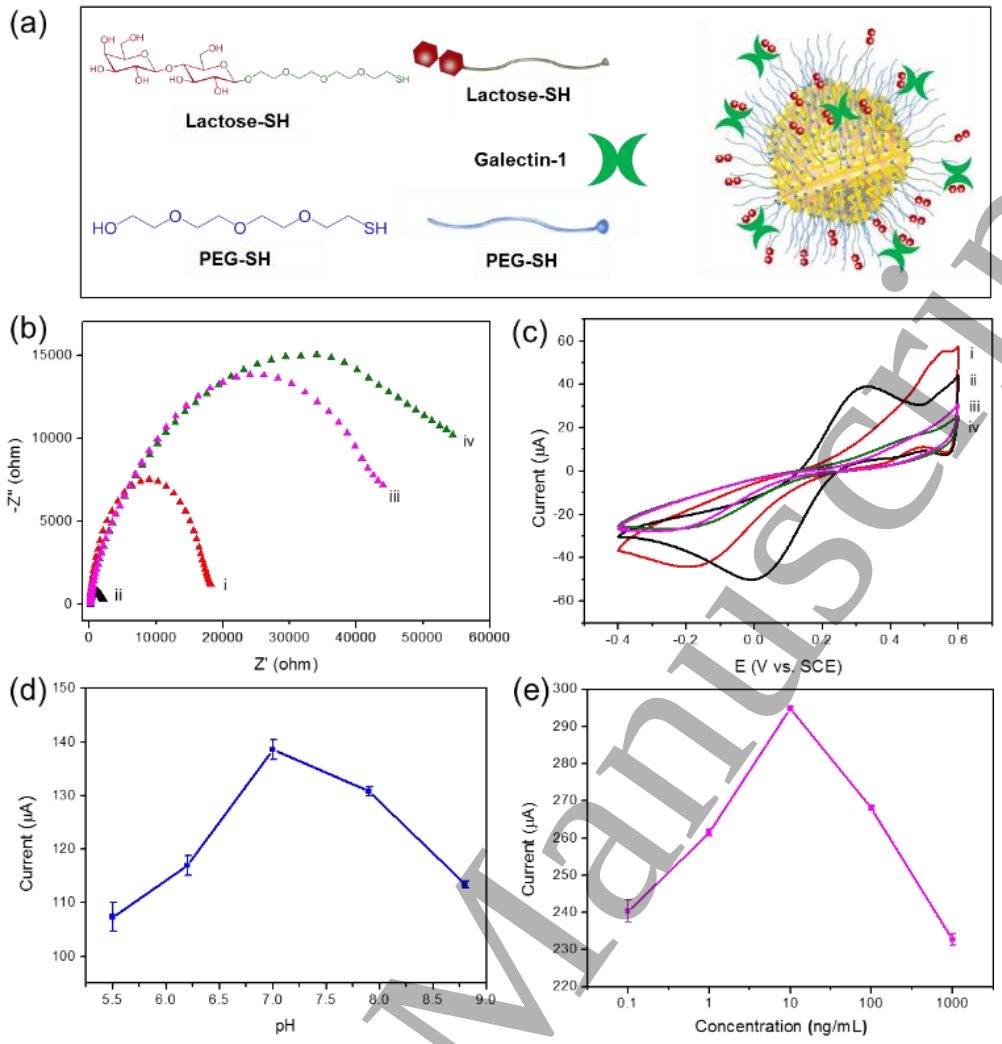

Figure 4. (a) Schematic illustration of the Cu_2O@Au/Lactose-SH/PEG-SH biosensor for Gal-1 recognition; (b) EIS and (c) CV responses of different electrodes in 5 mM $K_3[Fe(CN)_6]$ and 0.1 M KCl : Cu_2O@Au (i), Cu_2O@Au/Lactose-SH (ii), Cu_2O@Au/Lactose-SH/PEG-SH(iii), Cu_2O@Au/Lactose-SH/PEG-SH/Gal-1(iv); (d) Effect of pH and (e) Lactose-SH concentration on the electrocatalytic current responses of biosensor towards PBS solution and that containing 5 mM $K_3[Fe(CN)_6]$ and 0.1 M KCl, respectively.

27.66 μA and 26.57 μA respectively, after the PEG-SH blocking (iii) and Gal-1 capturing onto the surface of electrode (iv). It indicates the efficiency of electron transfer has been inhibited. Both the CV and EIS results support the successful fabrication of proposed biosensor.

To optimize the analytical performance, the experimental conditions including the pH value of electrolyte and the concentration of Lactose-SH ligand are further investigated. The pH value of electrolyte can affect the amperometric responses of the transducing materials and the activity of biological proteins [11]. In this respect, PBS solutions with different pH values are employed in the CV measurements with the corresponding results shown in Figure S2a. According to the calibrated result shown in Figure 4d, the current signal increases from 107.36 to 138.56 μA with the pH value increasing from 5.6 to 7.0, and then decreases to 113.50 μA with the pH value further increasing to 8.8. It indicates that the optimal amperometric response can be obtained at the pH value of 7.0. Moreover, the proteins can maintain their bioactivity in this neutral condition [35], hence PBS at pH value of 7.0 is recognized as the optimized electrolyte. The amount of surface-modified Lactose-SH ligand is also vital to the performance of biosensors for capturing Gal-1. Figure S2b reveals the redox peaks of the biosensor with different concentration of Lactose-SH ligand at the voltage range of 0.4~1.0 V, and the corresponding amperometric responses are shown in Figure 3e. With the increase of Lactose-SH concentration from 0.1 ng/mL to 10 ng/mL, the current increases from 240.33 μA to 294.86 μA, and the current subsequently decreases to 232.73 μA when the concentration of Lactose-SH further increases to 1 μg/mL. It is evident that the optimal amperometric response is achieved at a concentration of 10 ng/mL, which is selected for the following studies.

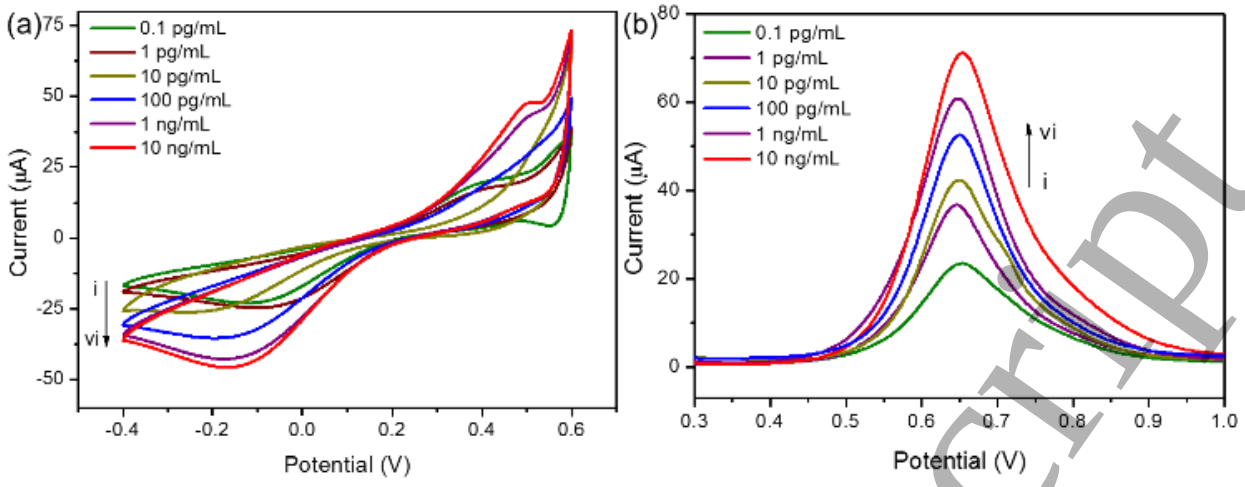

Figure 5. (a) CV and (b) DPV curves for the detection of Gal-1 with different concentrations: 0.1 pg/mL(i), 1 pg/mL(ii),10 pg/mL(iii), 100 pg/mL(iv), 1 ng/mL(v), 10 ng/mL(vi).

3.4. Analytical performances of the biosensor

Under the optimal experimental conditions, the prepared biosensor with Cu_2O@Au as signal amplification platform are further applied for the Gal-1 detection. By adding different concentrations of Gal-1, the CV and DPV responses are recorded to study the analytical performances of biosensor respectively. Figure 5a shows the representative relationship between CV redox peak current and the concentration of Gal-1. The redox peak current gradually increases with the increase of Gal-1 concentration from 0.1 pg/mL to 10 ng/mL. The average CV redox peak current obtained with three sets of measurements at different Gal-1 concentrations are shown in Figure S3, in which the error bars and linear fit demonstrate the reasonable detection reproducibility. Meanwhile, as shown in Figure 5b, the results of DPV measurement also indicate the increase of peak current after increasing the concentration of added Gal-1. The DPV measurement has also been conducted with the addition of 100 pg/mL bovine serum albumin (BSA) into the Gal-1 solution, and results in Figure S4 also exhibit the increase of the current peak with the increasing of Gal-1 concentration, which prelimarily indicates the specificity of the biosensor. Different from the previous study about the detection of Gal-1 based on the immunosensor [36], our results demonstrate the feasibility of electrochemical biosensor based on the galectin-lactose interaction, which can also be used for the rapid and exceptionally sensitive detection of Gal-1.

4. Conclusions

In this work, a novel kind of label-free electrochemical biosensor based on galectin-lactose interactions is successfully fabricated for the determination of tumor biomarker Gal-1. The lactose ligands on the surface of the prepared biosensor can capture Gal-1 and the detection signal is amplified by the catalytic performance of Cu_2O@Au nanocomposites substrate. According to the promising results for label-free detection of galectins, such simply and economical strategy may be valuable for the point-of-care early screening of cancers.

Acknowledgements

This work was jointly supported by Shenzhen Science and Technology Research Funding (Nos. JCYJ20160429190215470, JCYJ20160608141439330), Youth Innovation Promotion Association of Chinese Academy of Sciences (No. 2017416), Youth Talents of Guangdong Science and Technology Innovation (No. 2015TQ01C534), Science and Technology Service Network Initiative of Chinese Academy of Sciences (No. KFJ-STS-QYZX-035), Leading Talents of Guangdong Province Program (No. 00201520) as well as Shenzhen Peacock Program (No. KQTD2016030111500545).

ORCID iDs

Penghui Li https://orcid.org/0000-0001-7257-6381

References

[1] Duffy M J 2001 Clinical uses of tumor markers: A critical review Crit. *Rev. Clin. Lab. Sci.* **38** 225–62

[2] Compagno D, Jaworski F M, Gentilini L, Contrufo G, Perez I, Elola M T, Pregi N, Rabinovich G A and Laderach D J 2014 Galectins: Major signaling modulators inside and outside the cell *Curr. Mol. Med.* **14** 630–51

[3] Camby I, Le Mercier M, Lefranc F and Kiss R 2006 Galectin-1: A small protein with major functions *Glycobiology* **16** 137R–157R

[4] Arcolia V, Journe F, Wattier A, Leteurtre E, Renaud F, Gabius H-J, Remmelink M, Decaestecker C, Rodriguez, A, Boutry S, Laurent S, Saussez S 2017 Galectin-1 is a diagnostic marker involved in thyroid cancer progression *Int. J. Oncol.* **51** 760–70

[5] Chen L, Yao Y, Sun L, Zhou J, Liu J, Wang J, Li J and Tang J 2015 Clinical implication of the serum galectin-1 expression in epithelial ovarian cancer patients *J. Ovarian Res.* **8** 1–11

[6] Gomez-Brouchet A, Mourcin F, Gourraud P A, Bouvier C, De Pinieux G, Le Guelec S, Brousset P, Delisle M B and Schiff C 2010 Galectin-1 is a powerful marker to distinguish chondroblastic osteosarcoma and conventional chondrosarcoma *Hum. Pathol.* **41** 1220–30

[7] Martinez-Bosch N, Barranco L E, Orozco C A, Moreno M, Visa L, Iglesias M, Oldfield L, Neoptolemos J P, Greenhalf W, Earl J, Carrato A, Costello E and Navarro P 2018 Increased plasma levels of galectin-1 in pancreatic cancer: potential use as biomarker *Oncotarget* **9** 32984–96

[8] Orozco C A, Martinez-Bosch N, Guerrero P E, Vinaixa J, Dalotto-Moreno T, Iglesias M, Moreno M, Djurec M, Poirier F, Gabius H-J, Fernandez-Zapico M E, Hwang R F, Guerra C, Rabinovich G A and Navarro P 2018 Targeting galectin-1 inhibits pancreatic cancer progression by modulating tumor–stroma crosstalk *Proc. Natl. Acad. Sci. 115* E3769–78

[9] Kondo Y, Kishino M, Noda Y, Sakai M and Sato S 2016 Galectin-1 is a useful marker for detecting neoplastic squamous cells in oral cytology smears *Hum. Pathol.* **52** 101–9

[10] Jung E J, Moon H G, Bok I C, Jeong C Y, Joo Y T, Lee Y J, Hong S C, Choi S K, Ha W S, Jae W K, Lee C W, Jong S L and Park S T 2007 Galectin-1 expression in cancer-associated stromal cells correlates tumor invasiveness and tumor progression in breast cancer *Int. J. Cancer* **120** 2331–8

[11] Li F, Li Y, Feng J, Dong Y, Wang P, Chen L, Chen Z, Liu H and Wei Q 2017 Ultrasensitive amperometric immunosensor for PSA detection based on Cu_2O@CeO_2-Au nanocomposites as integrated triple signal amplification strategy *Biosens. Bioelectron.* **87** 630–7

[12] Zhang X, Li Y, Lv H, Feng J, Gao Z, Wang P, Dong Y, Liu Q and Zhao Z 2018 Sandwich-type electrochemical immunosensor based on Au@Ag supported on functionalized phenolic resin microporous carbon spheres for ultrasensitive analysis of α-fetoprotein *Biosens. Bioelectron.* **106** 142–8

[13] Feng T, Chen X, Qiao X, Sun Z, Wang H, Qi Y and Hong C 2016 Graphene oxide supported rhombic dodecahedral Cu_2O nanocrystals for the detection of carcinoembryonic antigen *Anal. Biochem.* **494** 101–7

[14] Liu F T and Rabinovich G A 2005 Galectins as modulators of tumour progression *Nat. Rev. Cancer* **5** 29–41

[15] Bian C C, Zhang Y, Li D F, Wang D C 2011 A Novel Binding Pattern Unique in Two Ligands for One Carbohydrate Recognition Domain in Galectins *Progress in Biochemistry and Biophysics* **38** 810–5

[16] S. A, H. K, H.-J. G, S. K, N. Y, C. F and K. K 1999 Galectins-1 and -3 and their ligands in tumor biology *J. Cancer Res. Clin. Oncol.* **125** 461–74

[17] Nesmelova I V., Ermakova E, Daragan V A, Pang M, Menéndez M, Lagartera L, Solís D, Baum L G and Mayo K H 2010 Lactose binding to galectin-1 modulates structural dynamics, increases conformational entropy, and occurs with apparent negative cooperativity *J. Mol. Biol.* **397** 1209–30

[18] Ansari A A, Kaushik A, Solanki P R and Malhotra B D 2008 Sol-gel derived nanoporous cerium oxide film for application to cholesterol biosensor *Electrochem. Commun.* **10** 1246–9

[19] Yang M, Li H, Javadi A and Gong S 2010 Multifunctional mesoporous silica nanoparticles as labels for the preparation of ultrasensitive electrochemical immunosensors *Biomaterials* **31** 3281–6

[20] Zhang S, Xia J and Li X 2008 Electrochemical biosensor for detection of adenosine based on structure-switching aptamer and amplification with reporter probe DNA modified Au nanoparticles *Anal. Chem.* 808382–8

[21] Lu J, Liu S, Ge S, Yan M, Yu J and Hu X 2012 Ultrasensitive electrochemical immunosensor based on Au nanoparticles dotted carbon nanotube-graphene composite and functionalized mesoporous materials *Biosens. Bioelectron.* **33** 29–35

[22] Won Y-H and Stanciu L A 2012 Cu_2O and Au/Cu_2O Particles: Surface Properties and Applications in Glucose Sensing *Sensors* **12** 13019–33

[23] Zou Z, Liu J, Yan X, Meng F and Gu J 2011 Nanoporous gold as non-enzymatic sensor for hydrogen peroxide *Electrochim. Acta* **56** 4657–62

[24] Cao X, Wang N, Jia S, Guo L and Li K 2013 Bimetallic AuPt nanochains: Synthesis and their application in electrochemical immunosensor for the detection of carcinoembryonic antigen *Biosens. Bioelectron.* **39** 226–30

[25] Xu Y T, Guo Y, Li C, Zhou X Y, Tucker M C, Fu X Z, Sun R and Wong C P 2015 Graphene oxide nano-sheets wrapped Cu_2O microspheres as improved performance

anode materials for lithium ion batteries *Nano Energy* **11** 38–47

[26] Zhao Y, Tong L, Li Y, Pan H, Zhang W, Guan M, Li W, Chen Y, Li Q, Li Z, Wang H, Yu X-F and Chu P K 2016 Lactose-Functionalized Gold Nanorods for Sensitive and Rapid Serological Diagnosis of Cancer *ACS Appl. Mater. Interfaces* **8** 5813–20

[27] Kuo C H and Huang M H 2008 Facile synthesis of Cu_2O nanocrystals with systematic shape evolution from cubic to octahedral structures *J. Phys. Chem. C* **112** 18355–60

[28] Chen S, Liu P, Su K, Li X, Qin Z, Xu W, Chen J, Li C and Qiu J 2018 Electrochemical aptasensor for thrombin using co-catalysis of hemin/G-quadruplex DNAzyme and octahedral Cu_2O-Au nanocomposites for signal amplification *Biosens. Bioelectron.* **99** 338–45

[29] Borgohain K, Murase N and Mahamuni S 2002 Synthesis and properties of Cu_2O quantum particles *J. Appl. Phys.* **92** 1292–7

[30] Liu X, Jian X, Yang H, Song X and Liang Z 2016 A photocatalytic graphene quantum dots-Cu_2O/bipolar membrane as a separator for water splitting *New J. Chem.* **40** 3075–9

[31] Zhao J, Sun L-W, Zou Y-C, Zhou L-J, Li G-D, Wang D-J, Feng L-L and Wang P-P 2013 Facile synthesis of highly stable and porous Cu_2O/CuO cubes with enhanced gas sensing properties *Sensors Actuators B Chem.* **188** 533–9

[32] Huang W C, Lyu L M, Yang Y C and Huang M H 2012 Synthesis of Cu_2O nanocrystals from cubic to rhombic dodecahedral structures and their comparative photocatalytic activity *J. Am. Chem. Soc.* **134** 1261–7

[33] Liu Y, Ma H, Gao J, Wu D, Ren X, Yan T, Pang X and Wei Q 2016 Ultrasensitive electrochemical immunosensor for SCCA detection based on ternary Pt/PdCu nanocube anchored on three-dimensional graphene framework for signal amplification *Biosens. Bioelectron.* **79** 71–8

[34] Ran X Q, Yuan R, Chai Y Q, Hong C L and Qian X Q 2010 A sensitive amperometric immunosensor for alpha-fetoprotein based on carbon nanotube/DNA/Thi/nano-Au modified glassy carbon electrode *Colloids Surfaces B Biointerfaces* **79** 421–6

[35] Katz E and Willner I 2005 Switching of directions of bioelectrocatalytic currents and photocurrents at electrode surfaces by using hydrophobic magnetic nanoparticles *Angew. Chemie Int. Ed.* **44** 4791–4

[36] Chuang C H, Du Y C, Wu T F, Chen C H, Lee D H, Chen S M, Huang T C, Wu H P and Shaikh M O 2016 Immunosensor for the ultrasensitive and quantitative detection of bladder cancer in point of care testing *Biosens. Bioelectron.* **84** 126–32